Why do many early-type galaxies lack emission lines? I. Fossil clues

Fabio Rafael Herpich, Grażyna Stasińska, Abílio Mateus, Natalia Vale Asari, Roberto Cid Fernandes

Monthly Notices
of the
ROYAL ASTRONOMICAL SOCIETY

MNRAS **481,** 1774–1785 (2018)
Advance Access publication 2018 September 3

doi:10.1093/mnras/sty2391

Why do many early-type galaxies lack emission lines? I. Fossil clues

F. Herpich,[1,2]★ G. Stasińska,[3] A. Mateus,[1] N. Vale Asari[1,4,5] and R. Cid Fernandes[1]

[1]*Departamento de Física–CFM, Universidade Federal de Santa Catarina, C.P. 476, 88040-900 Florianópolis, SC, Brazil*
[2]*Instituto de Astronomia, Geofísica e Ciências Atmosféricas, Universidade de São Paulo, R. do Matão 1226, 05508-090 São Paulo, Brazil*
[3]*LUTH, Observatoire de Paris, PSL, CNRS, UMPC, Univ Paris Diderot, 5 place Jules Janssen, F-92195 Meudon, France*
[4]*School of Physics and Astronomy, University of St Andrews, North Haugh, St Andrews KY16 9SS, UK*
[5]*Royal Society–Newton Advanced Fellowship, 6-9 Carlton House Terrace, London, SW1Y 5AG, UK*

Accepted 2018 August 30. Received 2018 August 30; in original form 2018 April 18

ABSTRACT

Early-type retired galaxies (RGs, i.e. galaxies which no longer form stars) can be divided into two classes: those with no emission lines, here dubbed lineless RGs, and those with emission lines, dubbed liny RGs. Both types of galaxies contain hot low-mass evolved stars (HOLMES) which emit ionizing photons. The difference must thus lie in the presence or absence of a reservoir of ionizable gas. From a volume-limited sample of 38 038 elliptical galaxies, we explore differences in physical properties between liny and lineless using data from the SDSS, WISE, and *GALEX* catalogues. To avoid biases in the comparison, we pair-match liny and lineless in stellar mass, redshift, and half-light Petrosian radius. We detect marginal differences in their optical stellar ages and NUV luminosities, indicating that liny RGs have an excess of intermediate-age (0.1–5 Gyr) stellar populations. Liny RGs show higher dust attenuation and *W*3 luminosities than their lineless counterparts. We also find that the amount of warm gas needed to explain the observed Hα luminosity in liny RGs is 10^5–10^8 $M_\odot$, and that their [N II]/[O II] emission-line ratios are typical of those of the most massive star-forming galaxies. Taken together, these results rules out the following sources for the warm gas in liny RGs: mass-loss from intermediate-mass stars, mergers with metal-poor galaxies and intergalactic streams. They imply instead an inflow of enriched gas previously expelled from the galaxy or a merger with a metal-rich galaxy. The ionization source and the origin of the gas producing the emission lines are thus disconnected.

Key words: galaxies: stellar content – galaxies: star formation – galaxies: elliptical and lenticular, cD – galaxies: evolution – galaxies: ISM.

1 INTRODUCTION

Until recently the text-book vision of early-type galaxies (ETGs) was that they are composed mostly of old stars and almost devoid of cold gas and dust. However, already five decades ago it was realized that a non-negligible fraction of them contained some gas, either neutral (e.g. Balkowski et al. 1972; Gallagher, Faber & Balick 1975) or ionized (Mayall 1958; Osterbrock 1960). It was also pointed out (e.g. Tinsley 1972) that continuous mass-loss from old stars could lead to the formation of younger generations of stars in ETGs. The far-ultraviolet excess observed in the central region of M31 (Code & Hoag 1969), first tentatively attributed to hot, highly evolved stars (Hills 1971), was later suggested to arise from hot young main-sequence stars (Tinsley 1971). Various ionization sources for the emission-line gas observed in elliptical galaxies were considered, such as decay of turbulence or ultraviolet radiation from hot stars (Osterbrock 1960).

In 1980, Heckman (1980) performed a systematic spectroscopic survey of the nuclei of nearby galaxies, and found that, while the nuclei of spiral galaxies often had spectra similar to H II regions, those of elliptical galaxies looked like the scaled-down version of the spectra of active galactic nuclei (AGN), with low luminosity and low excitation (but different from that of H II regions). He called those objects LINERs, for 'low ionization nuclear emission-line regions'. A wealth of hypothesis were proposed to explain the spectra of LINERs, such as nuclear activity (e.g. Ho, Filippenko & Sargent 1996; Barth et al. 2001; Filippenko 2003; Sabra et al. 2003; Chiaberge, Capetti & Macchetto 2005; Ricci, Steiner & Menezes 2015), shocks (Filippenko & Halpern 1984; Ho, Filippenko & Sargent 1993), young, massive stars (e.g. Filippenko & Terlevich 1992; Shields 1992; Ho & Filippenko 1993; Ho et al. 1996; Colina & Koratkar 1997; Alonso-Herrero et al. 2000; Eracleous et al. 2002; Rampazzo et al. 2005), or evolved low-mass stars (e.g. Stasińska et al. 2008; Annibali et al. 2010; Capetti & Baldi 2011; Yan & Blanton 2012,

★ E-mail: fabiorafaelh@gmail.com

2013; Singh, van de Ven & Jahnke 2014; Hsieh et al. 2017). There is still no consensus. The LINER problem has become one of the most discussed topics concerning galaxies with emission lines. In the 1990s, much progress had been achieved in the theoretical evolutionary synthesis of stellar populations, and some works described the spectral evolution of coeval stellar populations until very late stages where low-mass stars reached the white dwarf stage (Bruzual A. 1983; Bruzual A. & Charlot 1993; Fioc & Rocca-Volmerange 1997). Binette et al. (1994) then showed that the observed emission-line spectra in elliptical galaxies (for which data were still very scarce at that epoch) could well be explained by the ionization of hot, low-mass evolved stars (dubbed HOLMES[1] in later studies; e.g. Flores-Fajardo et al. 2011 and Cid Fernandes et al. 2011; hereafter CF11).

In the 2000s, the Sloan Digital Sky Survey (SDSS; York et al. 2000), which obtained imaging photometry and optical spectra for nearly one million galaxies, revolutionized the field of galaxy studies. At the same time, techniques were developed to analyse the stellar populations of the galaxies and extract the pure emission-line spectra from the observed one which included information on both the stellar populations and the interstellar gas (Cid Fernandes et al. 2005; Roig, Blanton & Yan 2015; Morelli et al. 2016). This allowed for the first time a correct determination of the emission-line spectra of ETGs and a panoramic view of the galaxy spectra in emission-line diagnostic diagrams (Kauffmann et al. 2003).

In the [O III]/Hβ versus [N II]/Hα plot (the so-called BPT diagram after Baldwin, Phillips & Terlevich 1981) the emission-line galaxies were cleanly separated between a 'star-forming' (SF) wing and a wing containing hosts of AGN. The lower part of the AGN wing was inappropriately labelled LINER (Kauffmann et al. 2003; Kewley et al. 2006), creating some confusion: in the SDSS, spectra were obtained through a 3 arcsec fibre, and for objects at redshifts larger than about 0.03, covered much more than the sole nucleus. Later, the denomination LIER (Belfiore et al. 2016) was proposed to underline that the spectra did not necessarily concern galaxy nuclei. In 2008, Stasińska et al. (2008) showed that ionization by the HOLMES inferred from the stellar population studies of the observed SDSS galaxies could well explain the LINER-type emission-line ratios observed for ETGs. In 2011, CF11 proposed a diagnostic diagram ($W_{\mathrm{H}\alpha}$ versus [N II]/Hα, dubbed the WHAN diagram) to distinguish true LINERs from galaxies ionized by their HOLMES [the so-called retired galaxies (RGs) introduced by Stasińska et al. 2008, meaning 'retired from their SF activity'].

2D spectroscopy, now available thanks to integral field units such as CALIFA and MaNGA (Sánchez et al. 2012 and Bundy et al. 2015, respectively) then confirmed that, in many cases, the WHAN diagram correctly distinguished RG from galaxies hosting a LINER in their nucleus (Sarzi et al. 2010; Singh et al. 2013; Gomes et al. 2016).

Presently, the widely accepted view of ETGs is that they contain an interstellar medium containing dust (Goudfrooij & de Jong 1995), neutral hydrogen with masses of 10^6–10^9 $\mathrm{M}_\odot$ (e.g. Krumm & Salpeter 1979; Goudfrooij et al. 1994; Oosterloo et al. 2010; Serra et al. 2012; Lagos et al. 2014; Woods & Gilfanov 2014), molecules (Combes, Young & Bureau 2007; Kaviraj et al. 2012; Davis et al. 2015), and have haloes of hot gas (Sarzi et al. 2013). They also contain emission-line zones extending out to several kiloparsecs (e.g. Sarzi et al. 2006; Singh et al. 2013; Woods & Gilfanov 2014; Gomes et al. 2016; Belfiore et al. 2017). HOLMES are one of the preferred options for the ionization of this gas.

This new and broadly consensual vision of the ETGs seems now to have occulted the old picture and perhaps diminished the interest in those ETGs that *do not present emission lines*. Some notable exceptions are the work by Rudnick et al. (2017), who studied a sample of ETGs with and without [O II] emission at redshifts between 0.4 and 0.8, and that by Belfiore et al. (2017), who analysed a sample of ETGs with MaNGA, looking for the reason behind the presence of gas and dust in some of these galaxies. As shown by CF11 and Stasińska et al. (2015), such objects constitute about half of the whole population of ETGs. They were dubbed *passive galaxies* (PG) in CF11, and *lineless retired* (LLR) in Herpich et al. (2016). Here we will call them 'lineless' RGs, by opposition to RGs with emission lines, which we will call 'liny' RGs.

As already shown by CF11, lineless and liny RGs have almost identical distribution of many physical parameters, such as (1) stellar mass; (2) optical colours; (3) stellar populations mean age and metallicity; etc. So how is it that such a large proportion of ETGs does not show emission lines at all? In this series of two papers we try to understand what makes a retired galaxy lineless or liny. More precisely, given that the stellar populations of both types of galaxies are very similar and have been shown to be able to produce a low-level ionization of their gaseous content, why is it that some RGs do not show any emission lines? In this paper, we look at the fossil properties of liny and lineless ETGs, meaning properties linked to their star formation history or to the chemical enrichment of their emission-line gas. In a companion paper (Mateus et al., in preparation), we will discuss environmental clues. We will attack our study by considering the information provided by three large surveys: SDSS in the optical, WISE (Wide-Field Infrared Survey Explorer) in the mid-infrared, and *GALEX* (Galaxy Evolution Explorer) in the UV.

This paper is organized as follows: Section 2 presents the data and sample selection; Section 3 presents a differential analysis of the stellar properties of the two classes of RGs that are the subject of this work; Section 4 discusses the origin of the gas in liny RGs; Section 5 puts together our findings; and finally Section 6 summarizes our results.

Throughout this work we adopt a flat cosmological model with Λcold dark matter (ΛCDM) with $H_0 = 70\,\mathrm{km\,s^{-1}\,Mpc^{-1}}$, $\Omega_M = 0.3$, and $\Omega_\Lambda = 0.7$.

2 DATA AND SAMPLES

We use the publicly available data from three large surveys, covering a spectral range from the ultraviolet to the infrared (SDSS, WISE, and *GALEX*; York et al. 2000; Wright et al. 2010; Martin et al. 2005). We also take advantage from two other projects: the spectral synthesis of stellar populations with the STARLIGHT code (Cid Fernandes et al. 2005) and the morphology analysis from the Galaxy Zoo (Lintott et al. 2008). In the following, we describe the surveys and explain our sample selection.

[1] We prefer the denomination of HOLMES to that of 'post-AGB stars' since in the stellar evolution community the latter term has for the last thirty years been used exclusively to designate the late stage of stellar evolution *previous* to the planetary nebula phase (see van Winckel 2003).

2.1 The data

We build our sample with the observations of the SDSS.[2] This survey took photometric and spectroscopic measures of a fourth of the sky in the visible range. The 7th Data Release (DR7; Abazajian et al. 2009) has photometric observations of about 350 million objects in five bands (*ugriz*), with effective wavelengths of 3551, 4686, 6165, 7481, and 8931 Å, respectively. SDSS DR7 has spectra of more than a million galaxies in the range from 3800 to 9200 Å, with mean spectral resolution of $\lambda/\Delta\lambda \sim 1800$ and obtained through fibres of 3 arcsec in diameter.

The WISE,[3] observed the entire sky in four bands of the mid-infrared, *W*1, *W*2, *W*3, and *W*4, with central wavelengths 3.4, 4.6, 12, and 22 μm, respectively. The All-Sky Data Release has positional data for more than 500 million objects with signal to noise SN > 5 to at least one band. The photometric calibration of WISE was made using the Vega system, and the conversion factor from Vega to AB is 2.683, 3.319, 5.242, and 6.604 for *W*1, *W*2, *W*3, and *W*4, respectively. We use this calibration to calculate WISE luminosities. However, as we do not directly compare WISE to SDSS magnitudes, we report WISE magnitudes in the Vega system.

The *GALEX* observed the whole sky in two ultraviolet photometric bands. Its 6th General Release (GR6) contains over 200 million photometric sources with measures in the far- and near-ultraviolet (FUV and NUV, respectively; Martin et al. 2005). The FUV band covers a spectral range from 1344 to 1786 Å, with a central wavelength of 1528 Å. The NUV band covers from 1771 to 2831 Å, with a central wavelength of 2310 Å (Bianchi, Conti & Shiao 2014). The *GALEX* mission performed a variety of surveys, the main one being the All Sky Survey (AIS), which covers an area of 26 000 square degrees with a magnitude limit of $m_{\rm AB} = 20.5$.

2.2 The sample

We start from a sample of 926 246 galaxies from SDSS-DR7 which have been analysed with the stellar population synthesis code STARLIGHT.[4] From those, we select only objects from SDSS Main Galaxy Sample, with half-light surface brightness $\mu_{50} \leqslant 24.5$ mag arcsec^{-2}, and absolute *r* magnitude $M_r \leq -20.43$. This gives us 553 316 objects. We match this sample to the MPA-JHU value-added catalogue to use their 'SPECTOFIBRE' parameter (i.e. to correct the SDSS-DR7 spectral flux calibration for extended sources, see http://www.mpa-garching.mpg.de/SDSS/DR7/raw_data.html). This sample is then matched to the Galaxy Zoo[5] catalogue, from which we obtain 515 320 galaxies.

In order to study retired ETGs removing red spirals or blue spirals with a 'retired' bulge, we select only those objects in the Galaxy Zoo catalogue for which the probability of being elliptical is higher than 0.5, and keep only the RGs (i.e. objects having $W_{\rm H\alpha} < 3$ Å which is the criterion defined by CF11), obtaining 168 786 objects.

We then remove all the objects for which the SDSS spectrum is not 'clean' in the region of the Hα line (e.g. containing bad pixels or sky lines) as described in Herpich et al. (2016) to guarantee that our lineless RG sample does not contain galaxies that might have unnoticed emission lines. We impose a signal-to-noise cut of $SN_{\rm H\alpha} > 3$ to liny RGs to select only those with reliable line measurements.[6] We thus obtain 59 662 liny RGs ($0.5 \leqslant W_{\rm H\alpha} < 3$ Å) and 96 844 lineless RGs ($W_{\rm H\alpha} < 0.5$ Å).

We then pair match the two RG samples in mass ($M_\star$), redshift (z), and half-light radius at *r* band (R_{50}), finding which liny best matches a given lineless RG. After excluding a few outliers (as detailed in Appendix A), we find 96 836 liny–lineless pairs. The mean absolute difference between pairs is $|\Delta \log M_\star| = 0.007$ dex, $|\Delta z| = 0.001$, and $|\Delta R_{50}| = 0.06$ kpc, with standard deviations of 0.018 dex, 0.003 and 0.19 kpc, respectively.

Finally, we select a volume limited sample (VLS) in the redshift range $0.04 < z < 0.095$, which contains 24 575 liny–lineless pairs, composed of 38 038 RGs (i.e. a liny RG can be a match to more than one lineless RG). This is our pair-matched optical VLS. We then define two other sub-samples: (1) the infrared sample using WISE data ($\rm SN_{W3} > 3$; WVLS), with 6944 pairs; and (2) the NUV sample using the NUV band from *GALEX* ($SN_{\rm NUV} > 3$; GVLS), with 8121 pairs. These three samples will be used throughout this work.

2.3 Stellar population analysis

The comparisons of liny and lineless RGs presented below are partly based on direct measurements and partly on properties derived from our STARLIGHT spectral fits. The latter were carried out using a set of 150 simple stellar populations (SSPs) from Bruzual & Charlot (2003), spanning six metallicities from $Z = 0.005$ to 2.5 $Z_\odot$, and 25 ages from 1 to 18 Gyr. The models use 'Padova 1994' evolutionary tracks and a Chabrier (2003) initial mass function. Extinction was modelled as due to a foreground screen following a Galactic reddening law with $R_V = 3.1$ (Cardelli, Clayton & Mathis 1989). This same setup was used in, for instance, Mateus et al. (2006), Mateus et al. (2007), Vale Asari et al. (2009), and CF11.

Of the properties derived from this analysis we will focus on the (fibre-corrected) stellar mass $M_\star$,[7] the stellar extinction A_V, the luminosity weighted mean stellar age $\langle t_\star \rangle$,[8] and the predicted rate of ionizing photons produced by populations older than 10^8 yr, $Q_{\rm HOLMES}$, as computed from the $\lambda < 912$ Å model spectra.

Uncertainties in these properties range from those related to noise in the data and the inversion method itself to others related to the ingredients (evolutionary tracks and spectral libraries) used in the analysis. Cid Fernandes et al. (2014) examines these issues in detail. Though the setup is not identical to the one used in our fits, their overall conclusions stand valid.

A key aspect of our study is that our comparison of liny and lineless systems is differential. By focusing on the differences in the stellar population properties among pairs of galaxies in these two families, we largely mitigate the effects of potential biases and uncertainties in the analysis. It is also worth noting that experiments

[2] http://www.sdss.org/

[3] http://www.nasa.gov/mission_pages/WISE/main/index.html

[4] http://starlight.ufsc.br

[5] http://www.galaxyzoo.org contains the morphological information for almost 900 thousand galaxies of the SDSS-DR7 (Lintott et al. 2008, 2011).

[6] This means that 12 277 galaxies cannot be stated to be either a liny or a lineless RG.

[7] $M_\star$ is the total stellar mass of the galaxy corrected for aperture effects by using the photometric *z*band fiber-to-total flux ratio, as in Kauffmann et al. (2003). We have verified that using the *r* band instead leads to the same masses to within ±0.05 dex. This extrapolation assumes no significant mass-to-light variations from the inner 3 arcsec to the galaxy as a whole, a hypothesis which is not critical for ETGs as those in our sample (González Delgado et al. 2015; Garcia-Benito et al. 2018, submitted).

[8] $\langle t_\star \rangle$ is actually defined as $\equiv 10^{\langle \log t_\star \rangle}$, where $\langle \log t_\star \rangle$ is the mean log age weighted by the contributions of different populations to the flux at normalization wavelength $\lambda_0 = 4020$ Å (see equation 2 of Cid Fernandes et al. 2005).

with more up-to-date SSP models confirm the results reported here (Werle 2018, in preparation).

Given our interest in the ionizing radiation field, it is relevant to point out that we deliberately ignore the predicted Lyman continuum from populations younger than 10^8 yr. This is done for several reasons. First, the ionizing photons output from young stars using spectral synthesis in the optical range is quite uncertain. The number of O stars in the stellar libraries we use is of just a few for all spectral types and metallicities, while the number of ionizing photons from individual O stars varies by almost two orders of magnitudes (Martins, Schaerer & Hillier 2005), making any interpolation difficult. In addition, the signatures of O stars in the optical range appear only in the blue part of the spectrum and are not very strong (Walborn & Fitzpatrick 1990). Finally they mostly rely on hydrogen and helium lines. The spectral region of hydrogen lines is removed from the synthesis done by STARLIGHT since it is affected also by emission from the interstellar medium. Therefore, the ionizing budget of young stellar populations cannot be derived accurately (a typical error of a factor of 2–4 is likely). Secondly, an optically insignificant contribution from $t \lesssim 10^7$ yr populations may well dominate the predicted $\lambda < 912$ Å flux, rendering the resulting predictions highly uncertain. For our galaxies we typically find that young stars account up to just 1.5 per cent of the flux at 4020 Å, but this irrelevant component is enough to make them ∼3 times brighter than old stars at ionizing energies. Thirdly, imperfect modeling of hot phases in the evolution of low-mass stars (like the horizontal branch) as well as blue stragglers (and possibly other effects associated to binary stars; e.g. Eldridge, Izzard & Tout 2008) may well lead spectral fitting codes like STARLIGHT to use young populations to compensate for the blue emission missing from old ones. This is what Ocvirk (2010) referred to as the 'fake young bursts' problem, where a genuinely old population is best fit by a mixture of an old and a young one due to these effects (see also Koleva et al. 2008; Cid Fernandes & González Delgado 2010).

3 DIFFERENTIAL ANALYSIS OF THE TWO RETIRED GROUPS

The two galaxy classes considered in this work are very similar, at least in the optical. And by construction our paired sample has galaxies which are even more similar. We show an example of the spectral features of liny and lineless RGs in Fig. 1. Each panel shows the observed stacked spectrum of lineless and liny RGs, as well the fit from the spectral synthesis and the observed minus model residual spectrum. The stacking was made selecting galaxies in a bin near the mean stellar mass ($\log M_\star/M_\odot = 11.16 \pm 0.10$), redshift ($z = 0.0705 \pm 0.0025$), and Petrosian radius ($R_{50} = 5.2 \pm 1.0$ arcsec) of our paired sample. This selection leaves us with 102 lineless–liny pairs; the bin limits were deliberately chosen to select little no more than a hundred pairs. The stacked spectra change very little regardless of the limits chosen.

3.1 Liny and lineless retired galaxies look the same...

Fig. 2 compares $Q_{\rm HOLMES}$, the total rate of hydrogen-ionizing photons produced by HOLMES, for liny and lineless RGs paired as explained in Section 2.2. The values of $Q_{\rm HOLMES}$ are obtained from the STARLIGHT decomposition of the galaxy spectra, counting only the photons produced by stellar populations older than 10^8 yr. In each category, the galaxies are grouped by stellar mass, $M_\star$, in bins of approximately the same number of objects. The curves are the median values of $Q_{\rm HOLMES}$ for each $M_\star$-bin as a function of $M_\star$. The

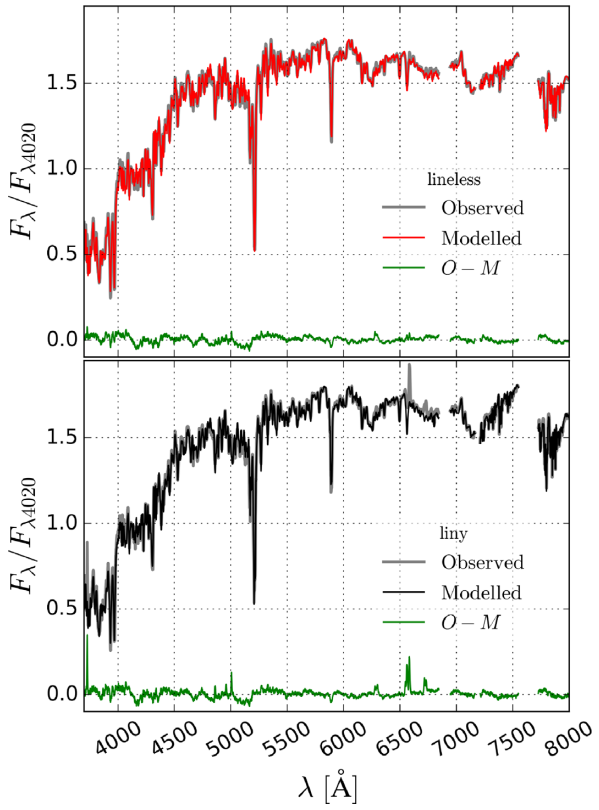

Figure 1. Upper panel: Observed lineless stacked spectrum using 102 lineless spectra (grey), the stacked model from STARLIGHT (red) and the residual spectrum observed minus modelled ($O-M$, green). Bottom panel: same as upper panel but for liny.

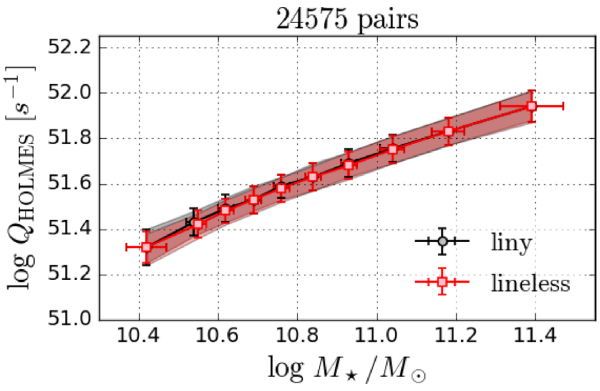

Figure 2. $Q_{\rm HOLMES}$, the rate of ionizing photons produced by stellar populations older than 10^8 yr versus the stellar mass of the galaxy. Liny RGs are in black and their matched lineless RGs in red. The markers are the median value for bins of mass containing approximately the same number of objects. The shadowed regions represent the quartiles of each distribution. The bars are the median absolute deviation to the median.

shadowed zones represent the quartiles of each distribution and the bars are the values for the median absolute deviation. Quantities in black refer to liny RGs and those in red to lineless RGs. In this plot, the black and red features cannot be distinguished, indicating that RGs of same stellar mass, observed at the same redshift, and with the fibre covering the same amount of galaxy light, produce exactly the same number of ionizing photons per second due to HOLMES, whether they show emission lines or not. This is due to the fact that,

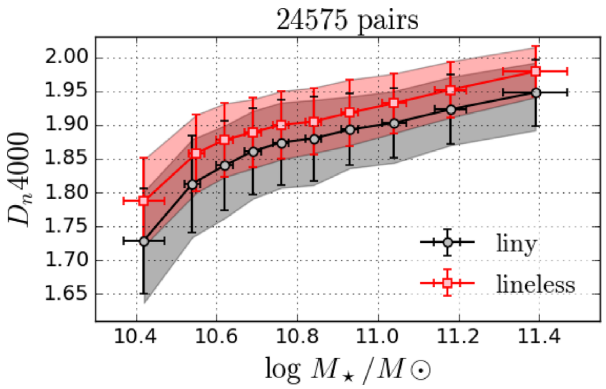

Figure 3. Same as Fig. 2 but for the D_n4000; break.

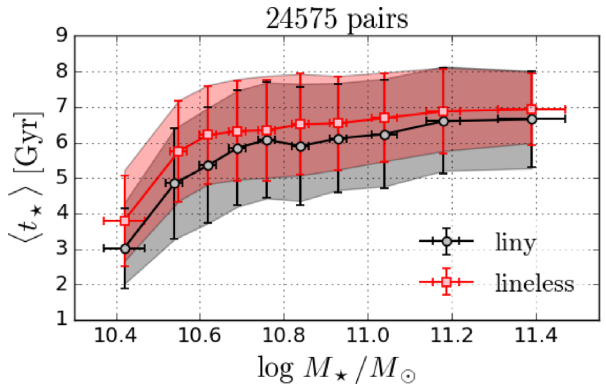

Figure 4. As Fig. 2 but for the mean stellar age weighted by light.

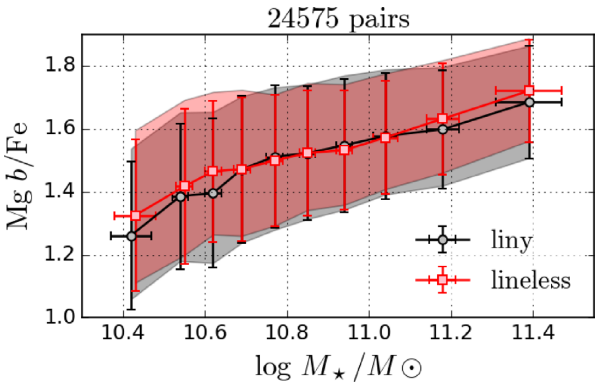

Figure 5. As Fig. 2 but for the α/Fe index Mg b/Fe where Fe stands for the mean flux of Fe$\lambda\lambda$5270, 5335.

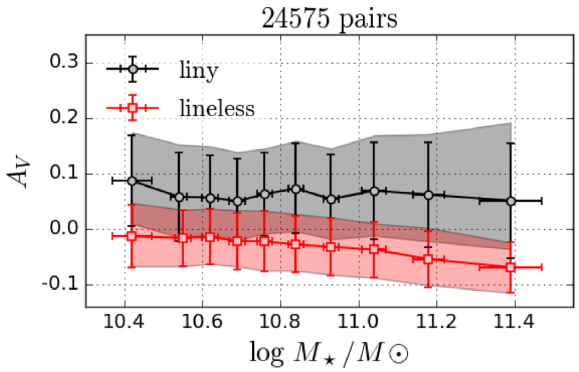

Figure 6. As Fig. 2 but for the attenuation obtained with the STARLIGHT A_V.

for a canonical stellar initial mass function, the ionizing photon production rate of HOLMES does not depend much on the detailed star formation history for look-back times larger than 10^8 yr (see fig. 2 of CF11). Thus liny and lineless RGs are not different in terms of the ionizing power of their HOLMES.

It is interesting to compare other aspects of the star formation histories of these two classes of galaxies. One is provided by the D_n4000 index (Balogh et al. 1999). This index is dependent on the mean age of the stellar population and – to a lesser extent – on their metallicities (Poggianti & Barbaro 1997), with larger values occurring for galaxies with older stellar populations. Fig. 3 shows that liny RGs tend to have slightly smaller values of D_n4000, at the verge of significance. Fig. 4 compares the flux-weighted stellar age $\langle t_\star \rangle$ as obtained by STARLIGHT between the two families. Here again liny RGs tend to show slightly smaller mean stellar ages. The effect is very small, but perceptible, contrary to the case of $Q_{\rm HOLMES}$, and occurs at all galaxy masses. These smaller ages cannot be due to ongoing star-formation, otherwise these galaxies would have a higher $W_{\rm H\alpha}$ and SF-like line ratios, contrary to what is observed. Instead, this result points to an excess of intermediate-age populations in liny with respect to lineless RGs.

An interesting feature in Figs 3 and 4 is that the differences in the stellar population ages between liny and lineless RGs tend to decrease toward larger galaxy masses. As we will see through this paper, this can be related with the limited amount of material that produces the emission lines. In such case, the effects produced either by the gas *per se*, or by a younger stellar population, are masked by the rest of the galaxy and become easier to notice in less massive ETGs. In summary, liny, and lineless RGs do not differ in their output of ionizing photons produced by HOLMES. They however seem to differ, on average, in their stellar populations of intermediate ages, but only slightly.

It is interesting to test whether these differences are somehow related to differences in α/Fe ratios among the two classes. Our SSP base models do not account for this effect, but empirical indices like Mg b/Fe (Thomas, Maraston & Bender 2003) can be used to tackle this issue. We have collected measurements of both Mg b and Fe[9] from the MPA/JHU catalogue (https://wwwmpa.mpa-garching.mpg.de/SDSS/DR7/SDSS_indx.html) and compared the alpha/Fe-sensitive Mg b/Fe ratio of liny and lineless. Fig. 5 shows the results and no difference is found.

3.2 ...but there are differences: dust

We now turn to indicators of the presence of dust. An obvious one is, of course, dust extinction. From STARLIGHT , it is possible to estimate the extinction of stellar light by interstellar grains, assuming that dust is distributed in a slab between the stars and the observer. This is of course not the situation encountered in ETGs. However, since the two families of galaxies considered are similar, it makes sense to investigate possible differences in A_V. Fig. 6 compares the values of A_V between the two families of RGs as a function of $M_\star$. Lineless RGs have values of A_V close to zero, while liny RGs have significantly higher values with a median value between 0.06 and 0.1. Negative values, encountered especially for lineless RGs, are obviously not physical. As discussed in Cid Fernandes et al. (2005), our spectral fits allow for $A_V < 0$ to account for

[9]Fe stands for the mean value of the flux for the λ5270 and λ5335 lines.

uncertainties in the flux calibration and Galactic extinction, as well as those associated with the modelling of dust attenuation itself.[10] It is worth noting that negative values of the extinction are also obtained without STARLIGHT , as in the study by Kauffmann et al. (2003). More importantly, imposing $A_V \geq 0$ does not erase the difference in A_V between liny and lineless RGs, which is the key result here.

Using Occam's razor argument, we may expect the extinction law to be similar for both families of galaxies. In that case, Fig. 6 indicates a larger amount of dust in the line of sight for liny galaxies. Qualitatively, this is precisely what is expected since liny galaxies contain warm gas which is likely mixed with some dust. Note that the estimated A_V does not necessarily allow a measure of the abundance of dust, since it was obtained under the hypothesis that the dust forms a screen between the stars and the observer.

Mid-infrared data, on the other hand, are able to directly detect the presence of hot dust. The *W*3 filter in WISE contains the polycyclic aromatic hydrocarbon (PAH) 11.2 and 12.7 μm features, which are greatly enhanced in the presence of the hard UV field able to excite the PAH grains (Draine & Li 2007). Fig. 7 compares WISE data for the two RG families. The top panel shows the behaviour of the $W2-W3$ colour. Liny RGs are clearly 'redder' than lineless ones. As the two bottom panels show, this difference in colour is due to an excess in the *W*3 band. Such an excess is generally interpreted as a sign of recent star formation, where the radiation field provided by the hot young stars excites the surrounding PAHs (Vermeij et al. 2002; Peeters, Spoon & Tielens 2004; Wu et al. 2005; Draine & Li 2007; da Cunha, Charlot & Elbaz 2008; Xu et al. 2015). But it could also be due to the presence of stars which have left the asymptotic giant branch and heat their expelled dust shells (Justtanont et al. 1996; Cassarà et al. 2013; Villaume, Conroy & Johnson 2015).

3.3 Other differences: UV

Ultraviolet data from GALEX can also give a clue on the nature of the stellar populations. The upper panel of Fig. 8 shows the behaviour of the NUV$-r$ colour. Liny RGs are clearly bluer than lineless ones and, as the bottom two panels show, this is entirely due to the luminosity in the NUV band. Because of their larger A_V's (Fig. 6), this stronger UV emission in linys becomes even more evident applying extinction corrections.

This indicates an excess population of intermediate age stars (0.1–5 Gyr) in liny RGs[11] (see also Kaviraj et al. 2007, 2011; Ko et al. 2013; Young et al. 2014). We note however that those stars are probably not the ones which ionize the emitting gas, as has sometimes been argued to reinforce the interpretation that a blue NUV$-r$ colour indicates ongoing star formation (Yi et al. 2005). Indeed, in all the liny RGs considered here, the ionizing radiation from the HOLMES is sufficient to explain the observed Hα luminosities. The ultraviolet difference observed here therefore does not trace the source of ionization

[10]The code allows for $A_V > -1$, but values bellow -0.2 occur in less than 3 per cent of our sample.

[11]An excess of HOLMES could also enhance the ultraviolet emission but from Fig. 2 the HOLMES populations are indistinguishable between liny and lineless RGs.

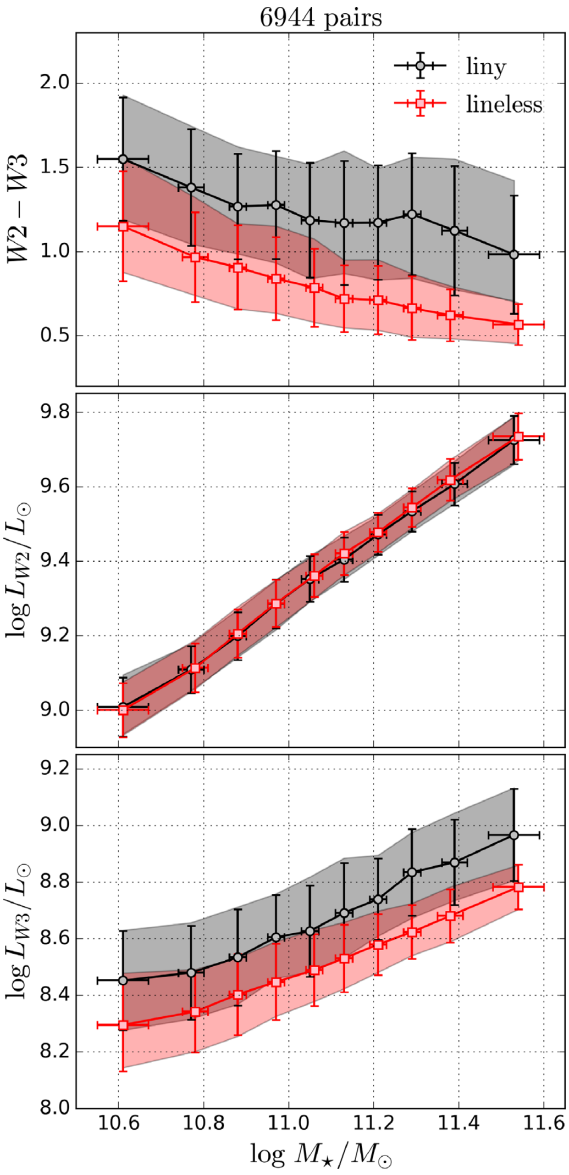

Figure 7. As Fig. 2 but comparing the WISE *W*3$-$*W*2 colour (top panel); *W*2 and *W*3 luminosities (middle and bottom panels, respectively).

(HOLMES), but the radiation emitted by middle-age main-sequence stars.

4 THE NATURE OF THE EMITTING GAS

The nature of the emitting gas in liny RGs is an important clue for what makes a retired galaxy liny or lineless. At first sight, one could think that the gas naturally comes from the stellar winds of intermediate mass stars, not only from previous stages of the HOLMES which provide the present-day ionizing radiation, but also that of stars which have not yet reached the stage of HOLMES and those which were initially more massive than the progenitors of present-day HOLMES.

The mass $M_{\mathrm{H}\alpha}$ of gas needed to produce the Hα luminosity in liny RGs can be obtained by combining the two equations

$$L_{\mathrm{H}\alpha} = \int n(H^+)\, n_{\mathrm{e}}\, \varepsilon_{\mathrm{H}\alpha}\, \mathrm{d}V, \qquad (1)$$

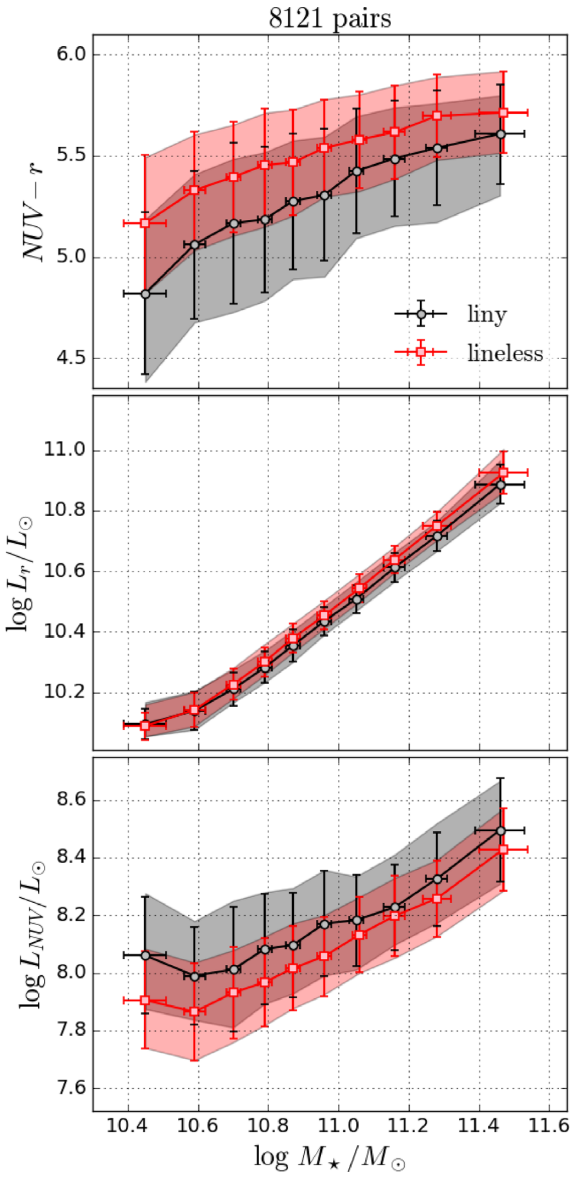

Figure 8. As Fig. 2 but for the NUV−r colour (top panel); L_r and the $L_{\rm NUV}$ (middle and bottom panel, respectively).

where $L_{\rm H\alpha}$ is the Hα luminosity, $n({\rm H}^+)$ and $n_{\rm e}$ are the H^+ and electron densities, $\varepsilon_{\rm H\alpha}$ is the Hα emissivity, and

$$M_{\rm H\alpha} = \int 1.4\, n({\rm H}^+)\, m_{\rm H}\, {\rm d}V, \qquad (2)$$

where $m_{\rm H}$ is the mass of an hydrogen atom. We obtain

$$\frac{M_{\rm H\alpha}}{L_{\rm H\alpha}} = \frac{1.4 m_{\rm H}}{\langle n_{\rm e}\rangle \varepsilon_{\rm H\alpha}}. \qquad (3)$$

where $\langle n_{\rm e}\rangle$ is an averaged electron density, which is not well known. Using $\langle n_{\rm e}\rangle = 0.1\,{\rm cm}^{-3}$, we find $M_{\rm H\alpha} \sim 10^8\,{\rm M}_\odot$. If we use the value found by Johansson et al. (2016) from stacked RG galaxy spectra, $\langle n_{\rm e}\rangle = 100\,{\rm cm}^{-3}$, this mass becomes $M_{\rm H\alpha} \sim 10^5\,{\rm M}_\odot$. This value is similar to that quoted by Davis & Bureau (2016) for local ETGs and by Pandya et al. (2017) for the most massive ETGs using the same $n_{\rm e} \sim 100\,{\rm cm}^{-3}$ density. Clearly the gas supplied by mass-loss from evolved stars (which is about the same as the present-day mass in stars) is more than enough to explain the observed Hα luminosities. This fact was already noted by Belfiore et al. (2017). Other options can be external gas from a recent merger or cooling filaments from galaxy haloes (e.g. Lagos et al. 2014, 2015; Davis & Bureau 2016).

The chemical composition of the emitting gas can give a hint as of to its origin. The metallicity cannot be measured with confidence by any 'strong-line method' because the physical conditions are certainly different from those for which the available methods were designed. One can instead use [N II]/[O II] as an indicator of the N/O ratio.[12] Since intermediate mass stars are the main source of nitrogen enrichment in massive galaxies (Mollá et al. 2015), the gas from their stellar winds should be, on average, extremely nitrogen-rich. There is no accurate way to measure whether the emitting gas in liny RGs is nitrogen-rich or not, because the N/O ratio in the interstellar medium of galaxies increases with their metallicity. What we can do is to compare the [N II]/[O II] ratios of liny RGs with those of SF galaxies of same mass or of same stellar metallicity (as derived from STARLIGHT).[13] This is done in Fig. 9, where liny RGs are represented in black and SF galaxies[14] in blue. The [N II]/[O II] ratios of SF galaxies are corrected for reddening using the observed Hα/Hβ ratio. For liny RGs, the Hβ line is seldom available.[15] In the top panels, the [N II]/[O II] values are not reddening corrected, considering that the extinction of the stellar light as derived from STARLIGHT is small (see Fig. 6). It can be seen that the [N II]/[O II] ratios of liny RGs are comparable with those of SF galaxies of same masses or metallicities, being on average larger by about 0.1 dex. If we consider that the nebular extinction in RGs is about five times larger than the stellar extinction, as obtained by Johansson et al. (2016) using stacked spectra, the intrinsic [N II]/[O II] ratios will be lower than they appear. In the bottom panels, we have corrected the observed values of [N II]/[O II] in RGs by multiplying the value of A_V derived from STARLIGHT by a factor of five. This lowers the [N II]/[O II] ratios of liny RGs by about 0.2 dex. If the gas emitting the [N II] and [O II] lines originated from mass-loss of intermediate-mass stars, one would expect a difference in [N II]/[O II] similar to the one between planetary nebulae and H II regions (i.e. about 0.7 dex from the data collected by e.g. Bresolin et al. 2010 or Stasińska et al. 2013). Thus we can definitely exclude that the emitting gas in liny RGs originates from stellar mass-loss.

This gas cannot come from mergers with low-metallicity galaxies either. Indeed, in Fig. 9, liny RGs are superimposed on the SF galaxies in the zone of common stellar masses, and extend the pattern observed for the SF galaxies to higher stellar masses with a similar slope. Therefore, the ratio [N II]/[O II] in liny RGs is similar to that of rather massive SF galaxies and at least 0.5 dex larger than in SF galaxies with masses smaller than $10^9\,{\rm M}_\odot$ as can be read from Fig. 9. This indicates that the emitting gas in liny RGs does not come from the merger with a metal-poor galaxy.

[12]The [N II]/[O II] ratio depends on N/O, on the metallicity and on the ionizing source.

[13]The fact that the ionizing radiation field from HOLMES is harder than that of SF regions have an impact on the [N II]/[O II] ratio, since the excitation potential of the [O II] line is higher than that of the [N II] line. But tests with photoionization models show that this effect is mild.

[14]The SF galaxies entering this figure are chosen from a VLS of the DR7-MGS with $0.04 < z < 0.095$ (similar as the VLS in Section 2). Additional constraints are SN > 3 for [O II], [N II] and Hα. The SF galaxies are selected after CF11, with $W_{\rm H\alpha} > 3$ Å and $\log$ [N II]/Hα < -0.4.

[15]In Fig. 9, we considered only objects for which the signal-to-noise ratio of the relevant line intensities is larger than three.

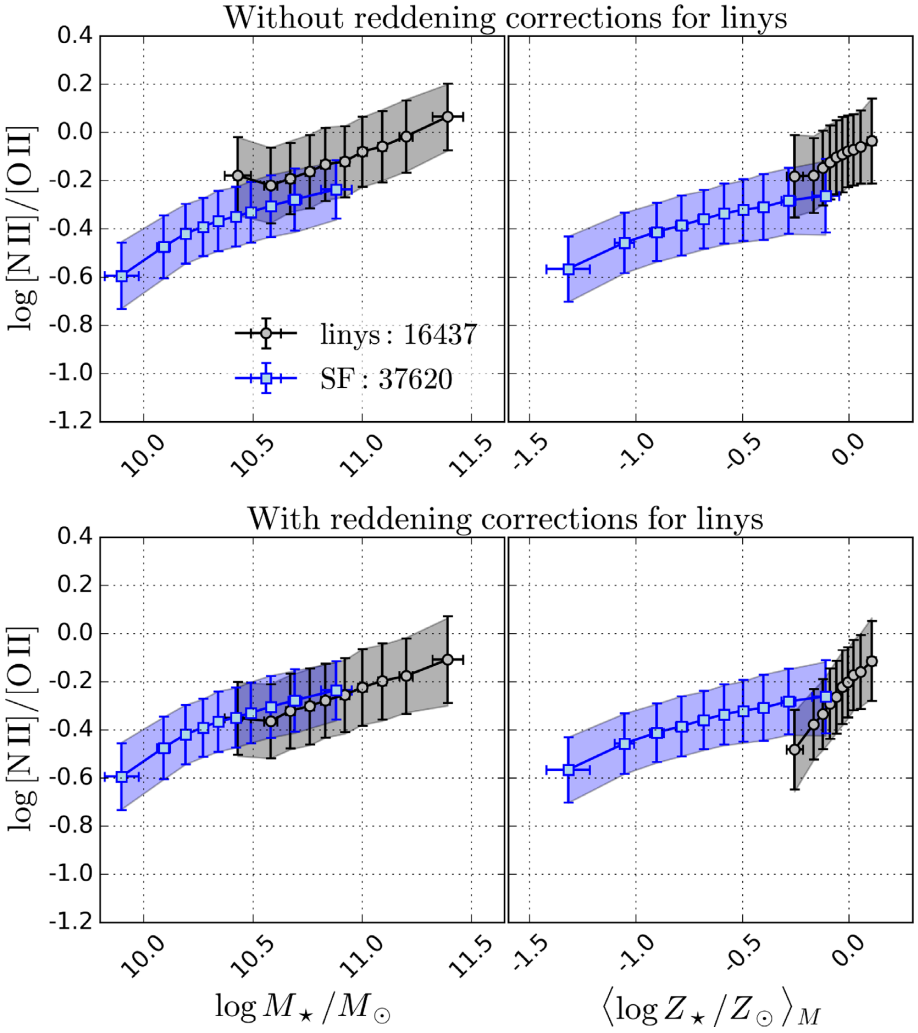

Figure 9. The ratio [N II]/[O II] as a function of the stellar mass (left-hand panels) and of the metallicity (right-hand panels) for SF galaxies (blue) and liny RGs (black). The markers represent the median for bins containing the same number of objects. The shadowed regions are the quartiles of both distributions and the bars represent the median absolute deviation. The emission lines of liny RG are displayed without reddening correction (upper panels) and with correction using $5 \times A_V$ (lower panels).

5 DISCUSSION

The broad conclusion from the previous sections is that, after a careful matching in stellar mass, redshift, and fibre covering fraction, we find that the HOLMES populations in liny RGs produce exactly the same number of ionizing photons as in the lineless ones (as shown by Fig. 2). We also note that the Hα luminosity from liny RGs is compatible with the photons produced by HOLMES populations. Following CF11, we define $\xi = L^{\rm obs}_{\rm H\alpha}/L^{\rm exp}_{\rm H\alpha}(t > 10^8\,{\rm yr})$, where $L^{\rm exp}_{\rm H\alpha}(t > 10^8\,{\rm yr})$ is the Hα luminosity expected from HOLMES. This parameter ξ should be $\leq$1 for galaxies whose ionizing spectra is powered by HOLMES (stellar populations with $t > 10^8$ yr), while any other source of the ionization, such as star formation or an active nucleus should produce a value $\xi \gg 1$. Fig. 10 shows that liny RGs do not need any source of ionization other than HOLMES. Note that, as a matter of fact, the distribution of the values of ξ peaks at $\log \xi = -0.4$, implying that a significant fraction of the ionizing photons produced by the HOLMES actually escapes even from liny RGs (Papaderos et al. 2013; Gomes et al. 2016).

We have shown, however, that liny RGs differ from the lineless ones by having slightly higher values of the stellar extinction A_V. This is not surprising since lineless RGs having no warm gas are also expected to be devoid of dust. Liny RGs have higher luminosities in the WISE *W*3 band and higher luminosities in the *GALEX* NUV band. Taken together, both facts point to a relatively recent period of star formation in liny RGs, which does not occur in lineless RGs. This is also detectable in the diagram showing D_n4000 (Fig. 3) as well as in the one showing the mean luminosity-weighted age derived from STARLIGHT (Fig. 4).

The gas out of which the stars formed and whose remnant is detectable through emission lines cannot come from stellar mass-loss in the old stellar populations, because, as seen in the previous section, it is not nitrogen-enriched. So it must have mainly an external origin. An additional argument for its origin could come from a comparison of the kinematics of the emission-line gas and that of the stars (e.g. Sarzi et al. 2006; Davis & Bureau 2016). The necessary information is not available in our SDSS data, but in a sample of about 50 LIER galaxies with extended emission from the MaNGA survey, (Belfiore et al. 2017) found that the distribution of the star-gas misalignment indicates an external origin of the emit-

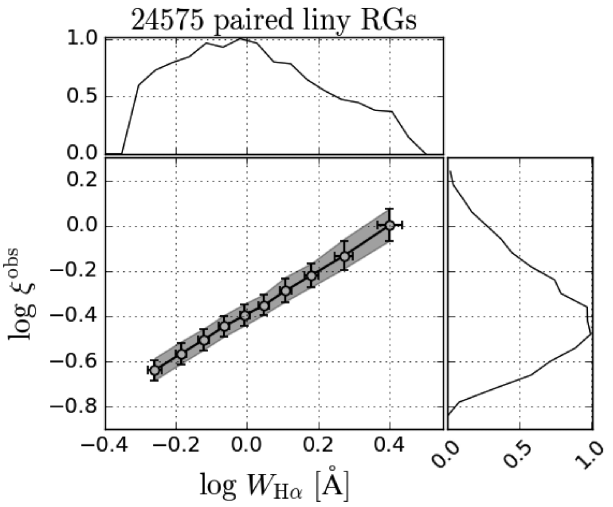

Figure 10. The equivalent width of H α versus ξ for liny RGs from our paired sample. The open circles are the median value of bins containing the same number of objects. The shadow region represents the quartiles of the distribution.

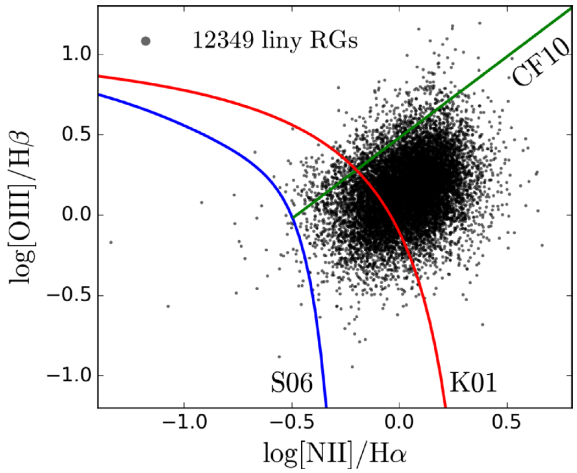

Figure 11. BPT diagram for the 12 349 liny RGs that survive the four-line SN cut. The blue line (S06) represents the pure-SF separation from Stasińska et al. (2006), the red one (K01) the so called 'upper starburst limit' from Kewley et al. (2001), and the green (CF10) is the Seyfert–LINER separation from Cid Fernandes et al. (2010).

ting gas (although they argue that internal processes may have a secondary role).

There are a number of studies that argue that a minor merger could be the cause of infrared and ultraviolet emission in many ETGs (e.g. Salim & Rich 2010; Kaviraj et al. 2011; Sheen et al. 2016). However, as seen in the previous section, the [N II]/[O II] ratio of liny RGs indicates that the impacting galaxies cannot be low-metallicity SF galaxies.

The only remaining possibilities that we can think of is that the emitting gas comes (i) from accretion from the haloes of the galaxies, (ii) from the intergalactic medium, or (iii) from residual streams of metal-rich gas coming from a merger in the recent past.

In the case of accretion from the haloes, one would a priori expect the emitting gas to be enriched in products from stellar mass-loss and supernova explosions (the so-called wind-recycling studied by van de Voort 2016). However, the analysis of the chemical composition of galactic haloes using X-rays or far-ultraviolet absorption spectra brought surprises and is not yet fully understood (Pipino & Matteucci 2011; Su & Irwin 2013; Prochaska et al. 2017). Besides there is presently no measurement of the N/O ratio in halo gas (and no theoretical estimate of it either). Anyway, from the point of view of the chemical composition, accretion from galactic haloes cannot presently be discarded to explain the emission lines in liny RGs. In the second scenario the gas in liny RGs would come from streams of cold gas found in the intergalactic medium, usually associated with galaxy groups or filaments (e.g. Sancisi et al. 2008; van de Voort & Schaye 2012). This looks less probable, since the intergalactic medium gas is expected to be very metal poor, $\sim 0.1 Z_{\odot}$, Danforth & Shull (2008), Oppenheimer et al. (2012), and van de Voort & Schaye (2012), which is far below what our most metal-poor liny RGs suggest (see Fig. 9). Finally, in the third scenario, cold gas comes from a merger episode with a metal-rich galaxy and now, a few billion years after the merger, it is slowly falling back to the galaxy. The first and third scenarios are the most probable for our liny RGs given the observed [N II]/[O II] ratios.

Our study indicates that liny RGs suffered an intermediate-age episode of star formation which is likely connected with the gas that is now being ionized by the HOLMES from the old stellar populations. Liny RGs *are not* ionized by young stellar populations since in the BPT diagram almost all are located well above the pure SF limit drawn by Stasińska et al. (2006), as seen in Fig. 11 which shows the values of [O III]/H β versus [N II]/H α (Baldwin et al. 1981) for our liny RGs. The figure plots only objects with SN > 3 for all four BPT emission lines, which drastically reduce the sample by a factor of five. Only 0.7 per cent of the RGs plotted in the figure are found inside the pure SF region. (Note that almost all the liny RGs live in the region previously attributed to LINER galaxies by Kauffmann et al. 2003, Kewley et al. 2006, etc.). It must be noted, however, that in some ETGs, massive ionizing stars may still be present, as indicated for e.g. by 2D studies of ETGs using CALIFA, which show zones where the H α equivalent width is of the order of 6–8 Å, therefore not attributable to HOLMES (Gomes et al. 2016).

Lineless RGs, on the other hand, did not suffer such recent episodes of star formation, and are thus devoid of cold gas. In a companion paper (Mateus et al., in preparation), we will look for environmental clues for their lack of gas.

A major point of concern is what happens to the gas ejected by stellar winds, which should be extensively observed in all RGs. The mass ejected back to the ISM is usually on order of the galaxy stellar mass ($\sim 4 \times 10^9 - 3 \times 10^{12}\,M_{\odot}$ for our sample). However, calculations show that gas from stellar mass-loss (Parriott & Bregman 2008) and planetary nebulae (Bregman & Parriott 2009) in ETGs is quickly heated to very high temperatures and it is not clear whether the amount of remaining warm gas is sufficient to explain the observed H α luminosities.

One can then ask why the same does not occur with the infalling gas. The dynamics of infalling gas is very different. Accretion timescales of infalling cold gas have been discussed by e.g. Davis & Bureau (2016) and argued to be long. The simulation of a test case of a massive ETG experiencing a major merger shows that a disc of gas misaligned with the stellar component is produced and persists for about 2 Gyr (van de Voort et al. 2015). Such conditions can allow the gas to live long enough for the emission lines be noticed.

6 SUMMARY

The main concern of this study was to find clues about why some RGs present emission lines and others do not. In this paper we

compared the physical properties of liny and lineless RG classes. In a volume-limited SDSS spectroscopic sample of ETGs, we pair-matched liny and lineless RGs in stellar mass, redshift, and R_{50} in order to avoid biases during the comparison procedure. We performed the comparison as a function of stellar mass and found the following:

(i) There is no difference in the ionizing photon budget of their old stellar populations ($Q_{\rm HOLMES}$). This means that both liny and lineless RGs have HOLMES capable of producing the same amount of Hα emission, so the difference between those two classes must lie in their warm gas content.

(ii) There is a systematic difference in D_n4000 and luminosity weighted mean stellar ages, indicating that liny RGs are younger on average, or have a younger component. Those differences are very small to be reliable on their own. Their significance is however reinforced by the excess NUV in liny RGs. This means that the small mean stellar age difference is not due to very young stars, but rather to intermediate-age stellar populations (0.1–5 Gyr).

(iii) Liny RGs have higher A_V and $W3$, which indicates either a difference in dust content or an enhanced population of HOLMES heating their expelled dust shells.

(iv) The amount of gas responsible for the Hα emission in liny RGs is smaller by orders of magnitude than the amount of matter ejected by winds from intermediate-mass stars. In other words, mass-loss from intermediate-mass stars would provide enough material to explain the Hα emission.

(v) The [N II]/[O II] emission-line ratio in liny RGs rules out the hypothesis that the line-emitting gas in RGs comes from stellar winds. It also rules out the hypothesis of metal-poor minor mergers being at the origin of this gas.

The overall conclusion of our work is that liny RGs must have experienced in the recent past an episode of star formation, and that the origin of the emission-line gas is either gas coming from the haloes of RGs (such as gas ejected in strong winds by massive OB stars or an AGN), or the left-over gas around the galaxy after the merger episode. The ionization of that gas would be due to HOLMES. On the other hand, lineless RGs would be RGs that did not experience such a recent merger or inflow of chemically enriched material.

We however note a problem: the hypothesis of a wet merger with a high-metallicity galaxy seems at odds with the current idea that ETGs in the Local Universe tend to grow via minor and gas-poor mergers (Naab, Johansson & Ostriker 2009; Conselice 2014; Kaviraj 2014). It is not clear whether this excludes the possibility of one merger with a metal-rich SF galaxy, such as modelled by Di Matteo et al. (2007). The hypothesis of enriched gas accreting from the haloes of the galaxies seems a priori less problematic. Simulations by Oppenheimer et al. (2010) show that late-time gas accretion and the resulting star formation is due to material previously expelled from the galaxy. However, as pointed out by those authors themselves and also by van de Voort (2016), such results depend on many issues not yet fully treated by the simulations.

A remaining question is what happens to the gas returned to the ISM by old stellar populations. In a typical massive ETG, the amount of ejected gas is about the same as its present-day stellar mass. Where does this gas go? There are a number of mechanisms which can explain the absence of warm gas in the ISM, usually involving a short time-scale ($t_d \sim 10^5$ yr) for gas destruction or heating. Kinematically disconnected gas, such as externally accreted gas, can survive longer and thus be ionized by HOLMES, emitting emission lines which embellish a liny RG's spectrum.

In a companion paper (Mateus et al. 2018, in preparation) we will present environmental factors linked to the presence or absence of emission lines in RGs, and discuss some possible scenarios that can explain the observations.

ACKNOWLEDGEMENTS

We thank the anonymous referee for the numerous suggestions that helped improve this work. F. R. Herpich thanks FAPESC and CAPES for the financial support during this work. The authors acknowledge the support from the CAPES CSF–PVE project 88881.068116/2014-01. NVA acknowledges support of the Royal Society and the Newton Fund via the award of a Royal Society–Newton Advanced Fellowship (grant NAF\R1\180403), and of FAPESC and CNPq. The Sloan Digital Sky Survey is a joint project of The University of Chicago, Fermilab, the Institute for Advanced Study, the Japan Participation Group, the Johns Hopkins University, the Los Alamos National Laboratory, the Max-Planck-Institute for Astronomy, the Max-Planck-Institute for Astrophysics, New Mexico State University, Princeton University, the United States Naval Observatory, and the University of Washington. Funding for the project has been provided by the Alfred P. Sloan Foundation, the Participating Institutions, the National Aeronautics and Space Administration, the National Science Foundation, the U.S. Department of Energy, the Japanese Monbukagakusho, and the Max Planck Society.

REFERENCES

Abazajian K. N. et al., 2009, ApJS, 182, 543
Alonso-Herrero A., Rieke M. J., Rieke G. H., Shields J. C., 2000, ApJ, 530, 688
Annibali F., Bressan A., Rampazzo R., Zeilinger W. W., Vega O., Panuzzo P., 2010, A&A, 519, A40
Baldwin J. A., Phillips M. M., Terlevich R., 1981, PASP, 93, 5
Balkowski C., Bottinelli L., Gouguenheim L., Heidmann J., 1972, A&A, 21, 303
Balogh M. L., Morris S. L., Yee H. K. C., Carlberg R. G., Ellingson E., 1999, ApJ, 527, 54
Barth A. J., Ho L. C., Filippenko A. V., Rix H.-W., Sargent W. L. W., 2001, ApJ, 546, 205
Belfiore F. et al., 2016, MNRAS, 461, 3111
Belfiore F. et al., 2017, MNRAS, 466, 2570
Bianchi L., Conti A., Shiao B., 2014, Adv. Space Res., 53, 900
Binette L., Magris C. G., Stasińska G., Bruzual A. G., 1994, A&A, 292, 13
Bregman J. N., Parriott J. R., 2009, ApJ, 699, 923
Bresolin F., Stasińska G., Vílchez J. M., Simon J. D., Rosolowsky E., 2010, MNRAS, 404, 1679
Bruzual A. G., 1983, ApJ, 273, 105
Bruzual A. G., Charlot S., 1993, ApJ, 405, 538
Bruzual G., Charlot S., 2003, MNRAS, 344, 1000
Bundy K. et al., 2015, ApJ, 798, 7
Capetti A., Baldi R. D., 2011, A&A, 529, A126
Cardelli J. A., Clayton G. C., Mathis J. S., 1989, ApJ, 345, 245
Cassarà L. P., Piovan L., Weiss A., Salaris M., Chiosi C., 2013, MNRAS, 436, 2824
Chabrier G., 2003, PASP, 115, 763
Chiaberge M., Capetti A., Macchetto F. D., 2005, ApJ, 625, 716
Cid Fernandes R., González Delgado R. M., 2010, MNRAS, 403, 780
Cid Fernandes R., Mateus A., Sodré L., Stasińska G., Gomes J. M., 2005, MNRAS, 358, 363
Cid Fernandes R., Stasińska G., Schlickmann M. S., Mateus A., Vale Asari N., Schoenell W., Sodré L., 2010, MNRAS, 403, 1036
Cid Fernandes R., Stasińska G., Mateus A., Vale Asari N., 2011, MNRAS, 413, 1687

Cid Fernandes R. et al., 2014, A&A, 561, A130
Code A. D., Hoag A. A., 1969, PASP, 81, 848
Colina L. Koratkar A., Peterson B. M., Cheng F.-Z., Wilson A. S., 1997, eds, ASP Conf. Ser. Vol. 113, IAU Colloq. 159: Emission Lines in Active Galaxies: New Methods and Techniques. Astron. Soc. Pac., San Francisco, p. 477
Combes F., Young L. M., Bureau M., 2007, MNRAS, 377, 1795
Conselice C. J., 2014, ARA&A, 52, 291
da Cunha E., Charlot S., Elbaz D., 2008, MNRAS, 388, 1595
Danforth C. W., Shull J. M., 2008, ApJ, 679, 194
Davis T. A., Bureau M., 2016, MNRAS, 457, 272
Davis T. A. et al., 2015, MNRAS, 449, 3503
Di Matteo P., Combes F., Melchior A.-L., Semelin B., 2007, A&A, 468, 61
Draine B. T., Li A., 2007, ApJ, 657, 810
Eldridge J. J., Izzard R. G., Tout C. A., 2008, MNRAS, 384, 1109
Eracleous M., Shields J. C., Chartas G., Moran E. C., 2002, ApJ, 565, 108
Filippenko A. V., 2003, in Collin S., Combes F., Shlosman I., eds, ASP Conf. Ser. Vol. 290, Active Galactic Nuclei: From Central Engine to Host Galaxy. Astron. Soc. Pac., San Francisco, p. 369
Filippenko A. V., Halpern J. P., 1984, ApJ, 285, 458
Filippenko A. V., Terlevich R., 1992, ApJ, 397, L79
Fioc M. Rocca-Volmerange B., Garzon F., Epchtein N., Omont A., Burton B., Persi P., 1997, eds, Astrophysics and Space Science Library. Vol. 210, The Impact of Large-Scale Near-IR Sky Surveys, Springer, Tenerife, Spain., p. 257
Flores-Fajardo N., Morisset C., Stasińska G., Binette L., 2011, MNRAS, 415, 2182
Gallagher J. S., Faber S. M., Balick B., 1975, ApJ, 202, 7
Gomes J. M. et al., 2016, A&A, 585, A92
González Delgado R. M. et al., 2015, A&A, 581, A103
Goudfrooij P., de Jong T., 1995, A&A, 298, 784
Goudfrooij P., de Jong T., Hansen L., Norgaard-Nielsen H. U., 1994, MNRAS, 271, 833
Heckman T. M., 1980, A&A, 87, 152
Herpich F., Mateus A., Stasińska G., Cid Fernandes R., Vale Asari N., 2016, MNRAS, 462, 1826
Hills J. G., 1971, A&A, 12, 1
Ho L. C., Filippenko A. V., 1993, Ap&SS, 205, 19
Ho L. C., Filippenko A. V., Sargent W. L. W., 1993, ApJ, 417, 63
Ho L. C., Filippenko A. V., Sargent W. L. W., 1996, ApJ, 462, 183
Hsieh B. C. et al., 2017, ApJ, 851, L24
Johansson J., Woods T. E., Gilfanov M., Sarzi M., Chen Y.-M., Oh K., 2016, MNRAS, 461, 4505
Justtanont K., Barlow M. J., Skinner C. J., Roche P. F., Aitken D. K., Smith C. H., 1996, A&A, 309, 612
Kauffmann G., Heckman T. M., White S. D. M., Charlot S., Tremonti C. et al., 2003, MNRAS, 341, 33
Kaviraj S., 2014, MNRAS, 437, L41
Kaviraj S. et al., 2007, ApJS, 173, 619
Kaviraj S., Tan K.-M., Ellis R. S., Silk J., 2011, MNRAS, 411, 2148
Kaviraj S. et al., 2012, MNRAS, 423, 49
Kewley L. J., Dopita M. A., Sutherland R. S., Heisler C. A., Trevena J., 2001, ApJ, 556, 121
Kewley L. J., Groves B., Kauffmann G., Heckman T., 2006, MNRAS, 372, 961
Ko J., Hwang H. S., Lee J. C., Sohn Y.-J., 2013, ApJ, 767, 90
Koleva M., Prugniel P., Ocvirk P., Le Borgne D., Soubiran C., 2008, MNRAS, 385, 1998
Krumm N., Salpeter E. E., 1979, ApJ, 228, 64
Lagos C. d. P., Davis T. A., Lacey C. G., Zwaan M. A., Baugh C. M., Gonzalez-Perez V., Padilla N. D., 2014, MNRAS, 443, 1002
Lagos C. d. P., Padilla N. D., Davis T. A., Lacey C. G., Baugh C. M., Gonzalez-Perez V., Zwaan M. A., Contreras S., 2015, MNRAS, 448, 1271
Lintott C. J. et al., 2008, MNRAS, 389, 1179
Lintott C. et al., 2011, MNRAS, 410, 166
Martin D. C. et al., 2005, ApJ, 619, L1
Martins F., Schaerer D., Hillier D. J., 2005, A&A, 436, 1049
Mateus A., Sodré L., Cid Fernandes R., Stasińska G., Schoenell W., Gomes J. M., 2006, MNRAS, 370, 721
Mateus A., Sodré L., Cid Fernandes R., Stasińska G., 2007, MNRAS, 374, 1457
Mayall N. U., 1958, in Roman N. G., ed., Proc. IAU Symp. 5. Comparison of the Large-Scale Structure of the Galactic System with that of Other Stellar Systems. Kluwer, Dordrecht, p. 23
Mollá M., Cavichia O., Gavilán M., Gibson B. K., 2015, MNRAS, 451, 3693
Morelli L., Parmiggiani M., Corsini E. M., Costantin L., Dalla Bontà E., Méndez-Abreu J., Pizzella A., 2016, MNRAS, 463, 4396
Naab T., Johansson P. H., Ostriker J. P., 2009, ApJ, 699, L178
Ocvirk P., 2010, ApJ, 709, 88
Oosterloo T. et al., 2010, MNRAS, 409, 500
Oppenheimer B. D., Davé R., Kereš D., Fardal M., Katz N., Kollmeier J. A., Weinberg D. H., 2010, MNRAS, 406, 2325
Oppenheimer B. D., Davé R., Katz N., Kollmeier J. A., Weinberg D. H., 2012, MNRAS, 420, 829
Osterbrock D. E., 1960, ApJ, 132, 325
Pandya V. et al., 2017, ApJ, 837, 40
Papaderos P. et al., 2013, A&A, 555, L1
Parriott J. R., Bregman J. N., 2008, ApJ, 681, 1215
Peeters E., Spoon H. W. W., Tielens A. G. G. M., 2004, ApJ, 613, 986
Pipino A., Matteucci F., 2011, A&A, 530, A98
Poggianti B. M., Barbaro G., 1997, A&A, 325, 1025
Prochaska J. X. et al., 2017, ApJ, 837, 169
Rampazzo R., Annibali F., Bressan A., Longhetti M., Padoan F., Zeilinger W. W., 2005, A&A, 433, 497
Ricci T. V., Steiner J. E., Menezes R. B., 2015, MNRAS, 451, 3728
Roig B., Blanton M. R., Yan R., 2015, ApJ, 808, 26
Rudnick G. et al., 2017, ApJ, 850, 181
Sabra B. M., Shields J. C., Ho L. C., Barth A. J., Filippenko A. V., 2003, ApJ, 584, 164
Salim S., Rich R. M., 2010, ApJ, 714, L290
Sánchez S. F. et al., 2012, A&A, 538, A8
Sancisi R., Fraternali F., Oosterloo T., van der Hulst T., 2008, A&A Rev., 15, 189
Sarzi M. et al., 2006, MNRAS, 366, 1151
Sarzi M. et al., 2010, MNRAS, 402, 2187
Sarzi M. et al., 2013, MNRAS, 432, 1845
Serra P. et al., 2012, MNRAS, 422, 1835
Sheen Y.-K., Yi S. K., Ree C. H., Jaffé Y., Demarco R., Treister E., 2016, ApJ, 827, 32
Shields J. C., 1992, ApJ, 399, L27
Singh R. et al., 2013, A&A, 558, A43
Singh R. van de Ven G. Jahnke K., Mickaelian A. M., Sanders D. B., 2014, eds, Proc. IAU Symp. 304. Multiwavelength AGN Surveys and Studies. Kluwer, Dordrecht, p. 280,
Stasińska G., Cid Fernandes R., Mateus A., Sodré L., Asari N. V., 2006, MNRAS, 371, 972
Stasińska G. et al., 2008, MNRAS, 391, L29
Stasińska G., Peña M., Bresolin F., Tsamis Y. G., 2013, A&A, 552, A12
Stasińska G., Costa-Duarte M. V., Vale Asari N., Cid Fernandes R., Sodré L., 2015, MNRAS, 449, 559
Su Y., Irwin J. A., 2013, ApJ, 766, 61
Thomas D., Maraston C., Bender R., 2003, MNRAS, 339, 897
Tinsley B. M., 1971, A&A, 15, 403
Tinsley B. M., 1972, ApJ, 178, 319
Vale Asari N., Stasińska G., Cid Fernandes R., Gomes J. M., Schlickmann M., Mateus A., Schoenell W., 2009, MNRAS, 396, L71
van de Voort F., 2016, MNRAS, 462, 778
van de Voort F., Schaye J., 2012, MNRAS, 423, 2991
van de Voort F., Davis T. A., Kereš D., Quataert E., Faucher-Giguère C.-A., Hopkins P. F., 2015, MNRAS, 451, 3269
van Winckel H., 2003, ARA&A, 41, 391

Vermeij R., Peeters E., Tielens A. G. G. M., van der Hulst J. M., 2002, A&A, 382, 1042
Villaume A., Conroy C., Johnson B. D., 2015, ApJ, 806, 82
Walborn N. R., Fitzpatrick E. L., 1990, PASP, 102, 379
Woods T. E., Gilfanov M., 2014, MNRAS, 439, 2351
Wright E. L. et al., 2010, AJ, 140, 1868
Wu H., Cao C., Hao C.-N., Liu F.-S., Wang J.-L., Xia X.-Y., Deng Z.-G., Young C. K.-S., 2005, ApJ, 632, L79
Xu L., Rieke G. H., Egami E., Haines C. P., Pereira M. J., Smith G. P., 2015, ApJ, 808, 159
Yan R., Blanton M. R., 2012, ApJ, 747, 61
Yan R. Blanton M. R., Thomas D., Pasquali A., Ferreras I., 2013, eds, Proc. IAU Symp. 295, The Intriguing Life of Massive Galaxies. Kluwer, Dordrecht, 328
Yi S. K. et al., 2005, ApJ, 619, L111
York D. G. et al., 2000, AJ, 120, 1579
Young L. M. et al., 2014, MNRAS, 444, 3408

APPENDIX A: THE PAIRING LINELESS VERSUS LINY

To guarantee a reliable description of the physical properties involved in our analysis, we draw a liny RG sample pair-matched to our lineness RG sample. To do this, we match the samples in three physical properties: the galaxy mass from STARLIGHT ($M_\star$), the redshift (z), and the Petrosian radius that contains half of the light of the galaxy in the r band (R_{50}). We use these parameters to find the most structurally similar pairs in our liny and lineless RG samples. Each one of these three properties is a parameter P that will be used to calculate the similarity between a lineless and a liny galaxy.

The methodology of the pair-matching procedure is quite simple: given a lineless RG galaxy, we compare each parameter P with the same parameter of those objects in the liny RG group. At the end, the liny galaxy with the smallest cumulative difference is chosen. Note that each lineless galaxy will be unique but the same is not necessarily true for liny RGs, as a single liny RG can be an ideal match to more than one lineless galaxy. Quantitatively, we compute the absolute value of the difference between the parameters P for a pair of galaxies, and normalize it by the standard deviation of P (σ_P) for all RGs in our sample. Finally, we sum the differences for all parameters P to obtain the similarity parameter SP:

$$SP_j = \sum_P \frac{|P^{\rm lineless} - P_j^{\rm liny}|}{\sigma_P}, \tag{A1}$$

where $P = \{\log M_\star, z, R_{50}\}$, $j = 1, 2, 3, \ldots, N$, and N is the total number of liny RGs.

We apply this procedure to our sample of 96 844 lineless and 59 662 liny RGs, described in Section 2.2. After this, each lineless at the list will have one ideal liny partner that minimizes SP. We then exclude outliers from the sample, choosing only pairs in which the value $|P^{\rm lineless} - P^{\rm liny}|$ is smaller than $3\sigma_P$, where $\sigma_{\log M_\star} = 0.357$ dex, $\sigma_z = 0.054$ and $\sigma_{R_{50}} = 2.493$ kpc, which excludes 8 pairs. Our paired sample is comprised of 96 836 parent lineless RGs that are paired with 41 286 unique liny RGs. From the pair-matched liny RGs, 17 617 are matched to only one lineless RG, 10 853 are matched to two lineless RGs, 5948 to 3, 2947 to 4, 1532 to 5, 2021 to 6–10, and 368 to more than 10 lineless RGs. The maximum number of lineless parents for a single liny RG is 103.

From those pairs, we select our volume-limited samples. The optical VLS sample has 24 575 lineless–liny pairs containing 13 463 unique liny RGs; the WVLS has 6944 pairs containing 4838 unique liny RGs; and the GVLS sample has 8121 lineless–liny pairs containing 5644 unique liny RGs.

This paper has been typeset from a TEX/LATEX file prepared by the author.